Heteroepitaxial growth of OPGaP on OPGaAs for frequency conversion in the IR and THz

Vladimir L. Tassev,[1,*] Shivashankar R. Vangala,[1,2] Rita D. Peterson,[1] Martin M. Kimani,[1,3] Michael Snure,[1] Ronald W. Stites,[1] Shekhar Guha,[1] Jonathan E. Slagle,[1] Trenton R. Ensley,[4,5] Akbar A. Syed,[4] and Ivan V. Markov[6]

[1]*Air Force Research Laboratory, Wright Patterson AFB, OH, 45433, USA*
[2]*SURVICE Eng. Co., Dayton, OH, 45431, USA*
[3]*WYLE, Aerospace Group, 909 W. Inyokern Rd Suite C, Ridgecrest, CA, 93555, USA*
[4]*CREOL, The College of Optics & Photonics, University of Central Florida, Orlando, FL, USA*
[5]*Current address: U.S. Army Research Laboratory, Adelphi, MD, 20783, USA*
[6]*Institute of Physical Chemistry, Bulgarian Academy of Sciences, Sofia, Bulgaria*
[*]*vladimir.tassev@wpafb.af.mil*

Abstract: For the first time thick orientation-patterned GaP (OPGaP) was repeatedly grown heteroepitaxially on OPGaAs templates as a quasi-phase matched medium for frequency conversion in the mid and longwave IR, and THz regions. The OP templates were fabricated by wafer-bonding and in a MBE-assisted polarity inversion process. Standard low-pressure hydride vapor phase epitaxy (LP-HVPE) was used for one-step growth of up to 400 μm thick device quality OPGaP with excellent domain fidelity. The presented results can be viewed as the missing link between a well-developed technique for preparation of OP templates, using one robust nonlinear optical material (GaAs), and the subsequent thick epitaxial growth on them of another material (GaP). The reason for these efforts is that the second material has some indisputable advantages in point of view of thermal and optical properties but the preparation of native templates encounters challenges, which makes it difficult to obtain high quality homoepitaxial growth at an affordable price. Successful heteroepitaxial growth at such a relatively high lattice mismatch (- 3.6%) in a close to equilibrium growth process such as HVPE is noteworthy, especially when previously reported attempts, for example, growth of OPZnSe on OPGaAs templates at about 10 times smaller lattice mismatch (+ 0.3%) have produced only limited results. Combining the advantages of the two most promising nonlinear materials, GaAs and GaP, is a solution that will accelerate the development of high power, tunable laser sources for the IR and THz region, which are in great demand on the market.

OCIS codes: (160.4330) Nonlinear optical materials; (230.7405) Wavelength conversion devices; (140.3070) Infrared and far-infrared lasers.

References and links

1. K. Thyagarajan, and A. Ghatak, *Lasers: Fundamentals and Applications* (Springer, 2011).
2. T. Maiman, "Stimulated Radiation in Ruby," Nature **187**(4736), 493–494 (1960).
3. T. Tacke, "Lead Laser Sources," Philos. Trans. R. Soc. Lond. A **359**(1780), 547–566 (2001).
4. H. Kildal and J. C. Mikkelsen, "The nonlinear coefficient phase matching and optical damage in the chalcopyrite $AgGaSe_2$," Opt. Commun. **9**(3), 315–318 (1973).
5. L. E. Myers and W. R. Bosenberg, "Periodically poled lithium niobate and quasi-phase matched optical parametric oscillators," IEEE J. Quantum Electron. **33**(10), 1663–1672 (1997).
6. A. Grisard, E. Lallier, and B. Gerard, "Quasi-phase-matched gallium arsenide for versatile mid-infrared frequency conversion," Opt. Mater. Express **2**(8), 1020–1026 (2012).
7. W. C. Hurlbut, Y. S. Lee, K. L. Vodopyanov, P. S. Kuo, and M. M. Fejer, "Multiphoton absorption and nonlinear refraction of GaAs in the mid-infrared," Opt. Lett. **32**(6), 668–670 (2007).

#259429 Received 16 Feb 2016; revised 15 Apr 2016; accepted 19 Apr 2016; published 27 Apr 2016

8. T. Skauli, P. S. Kuo, K. L. Vodopyanov, T. J. Pinguet, O. Levi, L. A. Eyres, J. S. Harris, M. M. Fejer, B. Gerard, L. Becouarn, and E. Lallier, "Improved dispersion relations for GaAs and applications to nonlinear optics," J. Appl. Phys. **94**(10), 6447–6455 (2003).
9. F. L. Madarasz, J. O. Dimmock, N. Dietz, and K. J. Bachmann, "Sellmeier parameters for $ZnGaP_2$ and GaP," J. Appl. Phys. **87**, 1564–1565 (2000).
10. I. Tomita, "Fabrication and characterization of a quasi-phase matched GaP optical device for terahertz-wave generation," Opt. Mater. **32**(2), 323–328 (2009).
11. T. Matsushita, I. Ohta, and T. Kondo, "Quasi-Phase-Matched Parametric Fluorescence in a Periodically Inverted GaP Waveguide," Appl. Phys. Express **2**, 0611011–0611013 (2009).
12. P. G. Schunemann, L. A. Pomeranz, and D. J. Magarrell, "Optical parametric oscillation in quasi-phase-matched GaP," Proc. SPIE **9347**, 93470J (2015).
13. L. A. Pomeranz, P. G. Schunemann, D. J. Magarrell, J. C. McCarthy, K. T. Zawilski, and D. E. Zelmon, "1-μm-pumped OPO based on orientation-patterned GaP," Proc. SPIE **9347**, 93470K (2015).
14. R. Peterson, D. Bliss, C. Lynch, and D. Tomich, "Progress in orientation-patterned GaAs for next-generation nonlinear optical devices," Proc. SPIE **6875**, 68750D (2008).
15. K. J. Bachmann, U. Rossow, N. Sukidi, H. Castleberry, and N. Dietza, "Heteroepitaxy of GaP on Si (100)," J. Vac. Sci. Technol. B **14**(4), 3019–3029 (1996).
16. T. Nakayama, "Electronic Structures of Heterovalent (001) Semiconductor Superlattices: GaP/ZnS and GaAs/ZnSe," J. Phys. Soc. Jpn. **61**(7), 2458–2468 (1992).
17. T. Nomura, Y. Maeda, M. Miyao, N. Hagino, and K. Ishikawa, "Accommodation of large lattice mismatch of GaP on GaAs (100) and GaAs on GaP (100) layers grown by MBE," Jpn. J. Appl. Phys. **26**(6), 908–911 (1987).
18. T. Soga, Y. Kohama, K. Uchida, M. Tajima, T. Jimbo, and M. Umeno, "MOCVD growth and characterization of GaAs and GaP on Si substrates," J. Cryst. Growth **91**(1-4), 499–503 (1988).
19. M. Ozeki, T. Haraguchi, T. Takeuchi, and K. Meada, "A comparative study of the growth mechanism of InAs/GaAs and GaP/GaAs heterostructures and strained layered super lattices by atomic layer epitaxy," J. Cryst. Growth **276**(3/4), 374–380 (2005).
20. C. C. Wang and S. H. McFarlane III, "Epitaxial growth and characterization of GaP on insulating substrates," J. Cryst. Growth **13**, 262–267 (1972).
21. W. G. Oldham, "Vapor growth of GaP on GaAs substrates," J. Appl. Phys. **36**(9), 2887–2890 (1965).
22. W. G. Spitzer, M. Gershenzon, C. J. Frosch, and D. F. Gibbs, "Optical absorption in n-type gallium phosphide," J. Phys. Chem. Solids **11**(3-4), 339–341 (1959).
23. D. A. Yasakov, A. N. Pikhtin, and V. I. Ulyanov, "Optical properties of gallium phosphide grown by floating zone," Mater. Res. Bull. **4**(11), 839–848 (1969).
24. V. Tassev, M. Snure, R. Peterson, R. Bedford, D. Bliss, G. Bryant, M. Mann, W. Goodhue, S. Vangala, K. Termkoa, A. Lin, J. S. Harris, M. M. Fejer, C. Yapp, and S. Tetlak, "Epitaxial growth of quasi-phasematched GaP for nonlinear applications: Systematic process improvements," J. Cryst. Growth **352**(1), 72–77 (2012).
25. V. Tassev, M. Snure, R. Peterson, K. L. Schepler, R. Bedford, M. Manna, S. Vangala, W. Goodhue, A. Lind, J. Harris, M. Fejer, and P. Schunemann, "Progress in orientation-patterned GaP for next-generation nonlinear optical devices," Proc. SPIE **8604**, 86040V (2013).
26. V. Tassev, M. Snure, S. Vangala, M. Kimani, R. Peterson, and P. Schunemann, "Growth and study of nonlinear optical materials for frequency conversion devices with applications in defense and security," Proc. SPIE **9253**, 925318 (2014).
27. V. Tassev, D. Bliss, C. Lynch, C. Yapp, W. Goodhue, and K. Termkoa, "Low pressure temperature gas flow HVPE growth of GaP for nonlinear optical frequency conversion devices," J. Cryst. Growth **312**(8), 1146–1149 (2010).
28. V. Tassev, D. Bliss, M. Snure, G. Bryant, R. Peterson, R. Bedford, C. Yapp, W. Goodhue, and K. Termkoa, "HVPE growth and characterization of GaP on different substrates and patterned templates for frequency conversion devices," J. Eur. Opt. Soc. **6**, 110171 (2011).
29. H. Sang, M. Li, X. Yu, and J. Zhou, "Study of intensity-dependent nonlinear optical coefficients of GaP optical crystal at 800 nm by femtosecond pump-probe experiment," Chin. Opt. Lett. **4**(9), 536–538 (2006).
30. F. Liu, Y. Li, Q. Xing, L. Chai, M. Hu, C. Wang, Y. Deng, Q. Sun, and C. Wang, "Three-photon absorption and Kerr nonlinearity in undoped bulk GaP excited by a femtosecond laser at 1040 nm," J. Opt. **12**, 095201 (2010).
31. K. Termkoa, S. Vangala, W. Goodhue, R. Peterson, R. Bedford, V. Tassev, C. Lynch, and D. Bliss, "Orientation-patterned GaP using wafer fusion technique," Opt. Mater. **34**, 30–35 (2011).
30. F. Liu, Y. Li, Q. Xing, L. Chai, M. Hu, C. Wang, Y. Deng, Q. Sun, and C. Wang, "Three-photon absorption and Kerr nonlinearity in undoped bulk GaP excited by a femtosecond laser at 1040 nm," J. Opt. **12**(9), 095201 (2010).
31. K. Termkoa, S. Vangala, W. Goodhue, R. Peterson, R. Bedford, V. Tassev, C. Lynch, and D. Bliss, "Orientation-patterned GaP using wafer fusion technique," Opt. Mater. **34**, 30–35 (2011).
32. S. R. Vangala, V. Tassev, M. Kimani, M. Snure, and R. Peterson, "Development of Thick Orientation Patterned GaP for Frequency Conversion in the Mid IR and THz Region," Proc. IRMMW-THz M **5**, 12.3 (2014).
33. B. A. Joyce and D. D. Vvedensky, "Self-organized growth on GaAs surfaces," Mater. Sci. Eng. **46**(6), 127–176 (2004).

#259429 Received 16 Feb 2016; revised 15 Apr 2016; accepted 19 Apr 2016; published 27 Apr 2016

34. N. Singh, G. Kanner, A. Berghmans, D. Kahler, A. Lin, B. Wagner, S. Kelley, D. Knuteson, R. Holmstrom, K. Schepler, R. Peterson, M. Fejer, and J. Harris, "Characteristics of thick ZnSe films on quasi-phase-matched (QPM) GaAs substrates," J. Cryst. Growth **312**(8), 1142–1145 (2010).
35. I. Markov, *Crystal Growth for Beginners* (World Scientific, 2008).
36. O. Pierre-Louis, M. R. D'Orsogna, and T. L. Einstein, "Edge Diffusion during Growth: The Kink Ehrlich-Schwoebel Effect and Resulting Instabilities," Phys. Rev. Lett. **82**(18), 3661–3664 (1999).
37. F. F. Leal, S. C. Ferreira, and S. O. Ferreira, "Modelling of epitaxial film growth with an Ehrlich-Schwoebel barrier dependent on the step height," J. Phys. Condens. Matter **23**(29), 292201 (2011).
38. D. B. Holt, "Misfit dislocations in semiconductors," J. Phys. Chem. Solids **27**(6-7), 1053–1067 (1966).
39. I. Markov and A. Milchev, "The effect of anharmonicity in epitaxial interfaces: Equilibrium structure of thin epitaxial films," Surf. Sci. **136**(2-3), 519–531 (1984).
40. A. Zangwill, *Physics at Surfaces* (Cambridge University Press, 1988).
41. H. Ibach, "Adsorbate-induced surface stress," J. Vac. Sci. Technol. A **12**(4), 2240–2246 (1994).
42. F. C. Frank and J. H. van der Merwe, "One-Dimensional Dislocations. III. Influence of the Second Harmonic Term in the Potential Representation, on the Properties of the Model," Proc. R. Soc. Lond. A Math. Phys. Sci. **200**(1060), 125–134 (1949).
43. V. Tassev and R. Peterson, Non-provisional patent "Heteroepitaxial Growth of Orientation-Patterned Materials on Orientation-Patterned Foreign Substrates," filed with the U.S. Patent and Trademark Office on Nov 06, 14934636 (2015).
44. V. Tassev and R. Peterson, Provisional patent "Heteroepitaxial Growth of Thick Orientation-Patterned GaP on Orientation-Patterned GaAs," filed with the U.S. Patent and Trademark Office on June 23, 62076520 (2015).
45. V. Tassev and R. Peterson, Provisional patent "Heteroepitaxial Growth of Thick Orientation-Patterned GaP on Orientation-Patterned GaAs," filed with the U.S. Patent and Trademark Office on Nov. 07, 62183208 (2014).

1. Introduction

High power, tunable, room temperature, compact and cost-effective laser sources in the IR and THz region are the perfect solution for a wide variety of military and civilian applications in areas such as defense (aircraft protection, laser radar, IR communications), security (airport scanners, remote sensing of chemicals and biological agents), industry (gas sensing, leak detection, pollution monitoring, process control), science (IR and THz spectroscopy) and medicine (medical imaging, biopsy-free cancer detection). Despite the large number of pulsed and continuous laser sources [1] developed since the first Ruby laser was demonstrated [2], there are only a few that can simultaneously cover both atmospheric transmission windows at 2–5 and 8–12 μm. These are the lasers based on ternary or quaternary lead salts ($Pb_xSn_{1-x}Te$ and $Pb_xEu_{1-x}Se_yTe_{1-y}$) [3] and the quantum cascade lasers (QCLs). However, the first ones rely on fairly small bandgap transitions and thus can produce modest output power of ~1 mW. Moreover, they are tunable over a few nm range only and require cryogenic temperatures to operate. Similarly, although that the QCLs can be made to operate at wavelengths from the near IR all the way to the THz region, they also have minimal tunability, low conversion efficiency, output power limited to about 5 W and performance that strongly deteriorates with increase in the temperature. To compensate the inability to achieve the needed wavelengths, power and tunability, using direct laser sources, some nonlinear frequency conversion processes, such as second harmonic generation (SHG), have been explored since the early 60s. This allowed the development of coherent sources based on three-wave mixing within a nonlinear medium. Converting the frequency of an available pump laser into a new wavelength of interest was first realized in bulk nonlinear birefringent crystals, such as $AgGaSe_2$, $ZnGeP_2$ [4] and KTP. However, limitations inherent to birefringent crystals, such as thermal lensing, damage, and beam walk-off, turned the attention to compensating the phase velocity dispersion by quasi-phase matching (QPM). QPM circumvents the constraint of birefringence, allowing the nonlinear material to be engineered to produce any wavelength within the whole transparency range of the material, and to take advantage of its largest element of the nonlinear susceptibility tensor $\chi^{(2)}$. The first practical realization of such a structure was in ferroelectric periodically-poled $LiNbO_3$ (PPLN), but its strong intrinsic absorption limited the use of this material only to wavelengths shorter than 4 μm [5]. In non-ferroelectric materials it is not possible to pattern the material through electric field poling. However, in such materials QPM still can be achieved by spatially inverting the nonlinear

#259429 Received 16 Feb 2016; revised 15 Apr 2016; accepted 19 Apr 2016; published 27 Apr 2016

susceptibility during growth. Recent advances in the planar technology allowed the fabrication of such thin microstructured materials, orientation-patterned (OP) templates, with the necessary domain reversal for QPM interaction. The last remaining step was to grow on these templates layers that are thick enough for bulk frequency conversion devices, while maintaining the periodic orientation of the initial template pattern.

Several different nonlinear optical (NLO) semiconductor materials are currently at different stages of development. GaAs with its broad IR transparency, high nonlinear optical susceptibility and mature growth technology has been highly successful as an OP nonlinear material [6] achieving over 60% slope efficiency in an optical parametric oscillator (OPO) device. Still, OPGaAs is not without limitations, chief among them its strong two-photon absorption (2PA) at wavelengths below 1.7 μm [7]. Thus a number of mature commercial lasers operating between 1 and 1.7 μm, for example, the Nd, Yb, and Er doped YAG lasers or the semiconductor laser diodes radiating at 1.55 μm (currently used in fiber optic communications), practically cannot be used as pump sources for GaAs. Compared to GaAs, GaP, as Fig. 1(a) shows, has negligible 2PA in the same spectral region, larger thermal conductivity, lower thermal expansion, and a broad transparency range that starts conveniently in the visible region [7], all at the cost of a slightly lower nonlinear susceptibility. In addition, GaP has a smaller refractive index than GaAs. Thus, according to Eq. (1) the quasi-phasematching period Λ should be significantly larger for GaP than for GaAs [8, 9], which is shown also in Fig. 1(b).

$$\frac{1}{\Lambda} = \frac{n_p}{\lambda_p} - \frac{n_s}{\lambda_s} - \frac{n_i}{\lambda_i} \tag{1}$$

(p, s and i denote the pump, signal, and idler waves)

The larger the period Λ, the easier is to fabricate the template and maintain good domain fidelity during the subsequent thick HVPE layer growth on the template.

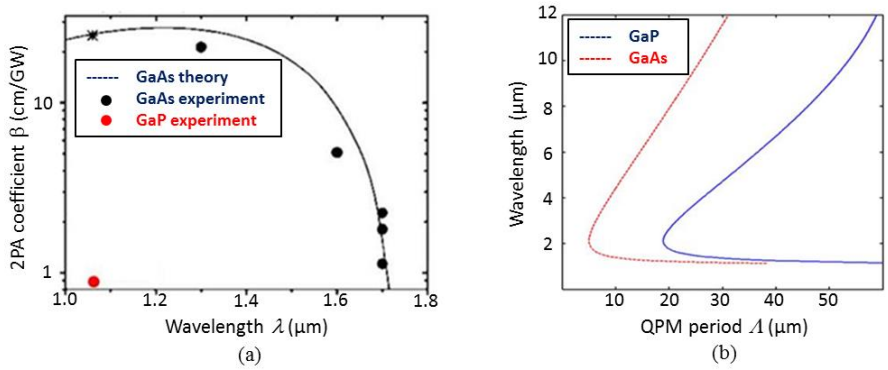

Fig. 1. 2PA of GaP (red dot-our measurement) compared to the 2PA of GaAs [7] (a); signal and idler wavelengths as a function of QPM period Λ for GaP and GaAs at a pump wavelength of 1.064 μm [8, 9] (b).

This rapidly increasing interest in GaP as an orientation-patterned QPM material led to the design of the first GaP frequency conversion device (FCD) based on stacked GaP wafers [10] and to the first demonstration of QPM parametric fluorescence in periodically inverted GaP [11]. OPO operation was also recently reported in OPGaP grown on native OPGaP templates, pumped at 2 μm [12] and at 1 μm [13]. However, performance remains modest with slope efficiency of 16% (compared with the 60% slope efficiency routinely obtained in OPGaAs [14]) and output power of 350 mW for the 2 μm case, and much less for the 1 μm case.

#259429 Received 16 Feb 2016; revised 15 Apr 2016; accepted 19 Apr 2016; published 27 Apr 2016

Obviously, significant improvement in material quality will be necessary in both fabrication of OP templates and subsequent thick growth on them in order to reap the benefits of the low 2PA of GaP at the shorter pump wavelengths. Some details discussed in the following paragraphs lead us to believe that combining the advantages of the two most promising materials, GaP and GaAs, in an attempt to grow heteroepitaxially OPGaP on OPGaAs templates would be worthy. In fact, heteroepitaxy of GaP and GaAs on foreign substrates (Si [15], ZnS [16], ZnSe [16], CaF_2, etc.), including growth on each other [17] have been already attempted using different growth techniques such as MOCVD [18] MBE [17], or ALE (atomic layer epitaxy) [19]. However, they can only provide thin films of up to 1 to 2 um thickness. Only HVPE is capable of producing hundreds of microns thick layers. As a starting point, some earlier studies indicated that homoepitaxial GaP grows much slower than GaAs [20] and with poorer crystalline quality [21]. At the same time all available n-type GaP samples possess an additional absorption band between 2 and 4 μm [22, 23]. Some of these shortcomings were addressed during earlier stages of this research [24–28]. Other challenges remained, however, and thus left room for improvements by heteroepitaxy.

2. The experiment: procedures and results

2.1. HVPE growth: System configuration and basic growth conditions

All HVPE growths of GaP were performed in a hot wall horizontal quartz reactor customized for low pressure operation. The 3-inch diameter quartz tube was heated in a 4-zone resistive furnace. A quartz boat with metal Ga was placed in the first zone. HCl passing the molten Ga formed GaCl and delivered it to the middle (mixing) zone, where GaCl meets for the first time the peripheral (outer) PH_3 flow. In some cases AsH_3 or a PH_3/AsH_3 mixture were used instead of PH_3 only. The substrate(s) was (were) placed in the third (growth) furnace zone. The fourth zone was reserved to accommodate the parasitic nucleation of the excess chemical species that had not reacted in the growth process. High purity H_2 was used as a carrier gas in both inner and outer flows to dilute the precursors and to deliver the reactant species. More details about the process, including the reactor configuration and the applied growth parameters, such as reactor pressure, substrate and mixing zone temperature, and gas flow regimes are given in our previous works [24–28].

2.2. HVPE growth on plain GaP and GaAs substrates

Before growing on OP templates the homo and heteroepitaxial growths were performed first on plain (bare) “on-axis” (100) GaP and (100) GaAs wafers and on (100) wafers with 4° miscuts towards (111)B. It turned out that the growth on miscut substrates is faster and results in smoother surface morphology in comparison to the growth on “on-axis” substrates, where surface morphology revealed a number of 3D-hillock formations that can be seen in Fig. 2. At the same time, compared to the growth of GaP on GaP, shown in Fig. 2(a), the hillock growth of GaP on the GaAs substrates was not that intensive, i.e. the number of 3D-formations was smaller, as was their average height, as Fig. 2(b) shows. 3D-hillocks were rarely observed on layers grown on miscut wafers (not shown here). These surfaces were relatively smooth, often with “orange-peel” type texture, and in rare cases exhibited either etch-pits or stacking faults, both predominantly oriented in one direction.

#259429 Received 16 Feb 2016; revised 15 Apr 2016; accepted 19 Apr 2016; published 27 Apr 2016

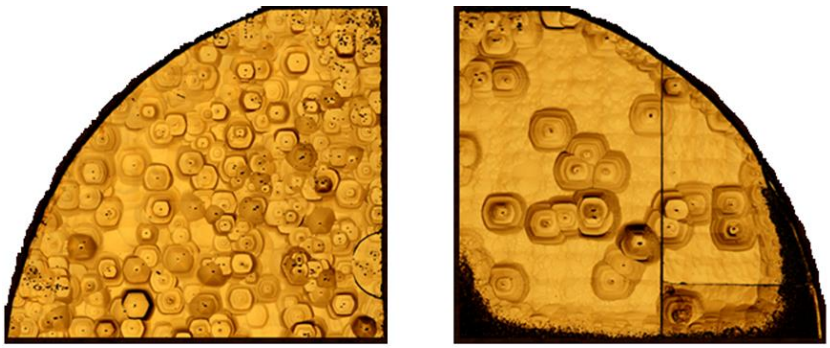

Fig. 2. Nomarski microscopy images (assembled by stitching software) of the top HVPE GaP surfaces grown on unpatterned "on-axis" (100) GaP (a) and GaAs (b) quarters of 2-inch wafers. The thicknesses of the two layers are slightly different but both are about 200 μm thick.

The explanation of the more intensive 3D hillock growth on the "on-axis" templates and the smoother surface morphology in growths on miscut templates is simple; a miscut surface provides more sites for the atoms approaching the growing surface to adhere at the monoatomic terraces, while an "on-axis" surface does not. In a close to equilibrium process such as the HVPE process, growth on such "on-axis" surfaces can start around surface defects, such as screw dislocations, which usually appear on the crystal surface as etch pits. That is why the etch pit density (EPD) of the material is an important factor for more or less intensive 3D growth. Comparing the EPD of the available on the market GaP and GaAs wafers (Table 1) one can be surprised by the much lower quality (larger EPD) of the GaP wafers. That is why the hillock growth after homoepitaxial growth of GaP on a GaP substrate, as Fig. 2(a) indicates, is more intensive and shows larger average surface roughness (RMS) than what we see after heteroepitaxy of GaP on a GaAs substrate (see Fig. 2(b)):

Table 1. A comparison of price and quality (EPD/cm^2) of commercial 2-inch GaP and GaAs.

Characteristics / Wafer material	GaP	GaAs
Price per 2-inch 2-side polished wafer [USD]	585–685	87–90
EPD [etch pits/cm^2]	80,000 –100,000	1,500–5,000*

*The data represent the ranges for price and EPD taken from several recent vendors' quotes.

A comparison of the FWHM (full width at half maximum) of the rocking curves obtained by omega-scan (omega is the source angle) x-ray diffraction (XRD) measurements before the HVPE growth confirmed also the expected higher crystalline quality of the commercially available GaAs wafers relative to the GaP wafers (Table 2). It was surprising, however, that again, despite the relatively large negative lattice mismatch between GaP and GaAs, - 3.6%, the FWHM (XRD omega-scan) of the GaP layer grown on GaAs was still comparable to the FWHM of GaP grown on GaP (Table 2):

Table 2. A comparison of the FWHM (XRD omega-scan) of GaP and GaAs wafers before and after the HVPE growth.

Before Growth		After Growth	
(100) GaP 4° [arcsec]	(100) GaAs 4° [arcsec]	GaP/GaP [arcsec]	GaP/GaAs [arcsec]
86	37	103	225

#259429 Received 16 Feb 2016; revised 15 Apr 2016; accepted 19 Apr 2016; published 27 Apr 2016

Growths conducted on bare "on-axis" and miscut GaP and GaAs substrates were then compared in order to determine the optimal conditions for growth on the OP-templates. The growths of GaP on plain GaAs and of GaAs on plain GaP were conducted at different growth conditions, including at different PH_3/AsH_3 ratios with the intention to create an intermediate GaAsP buffer layer. In these cases mutual diffusion of P and As was detected towards both the substrate and the growing layer. This process, revealed by elemental EDS (Energy Dispersive Spectroscopy)-profile, showed that even when the phosphine/arsine ratio was set constant the composition of $GaAs_xP_{x-1}$ within the growing layer is changing gradually with the distance from the interface. This gradual change continues until the composition demanded by the set PH_3/AsH_3 ratio is achieved at a distance from the substrate that can be called "critical", as the structure remains crystalline throughout the whole transition from one material to the other. Mutual diffusion of As and P was detected even when no attempts were made to grow an intermediate buffer layer. Thus, with optimization of the reactor configuration and the process parameters, up to 500–600 μm thick GaP and GaAs layers with smooth surface morphology and high crystalline quality have been repeatedly grown homo- and heteroepitaxially on both GaP and GaAs substrates. Figure 3 particularly shows heteroepitaxy of GaP on GaAs substrate.

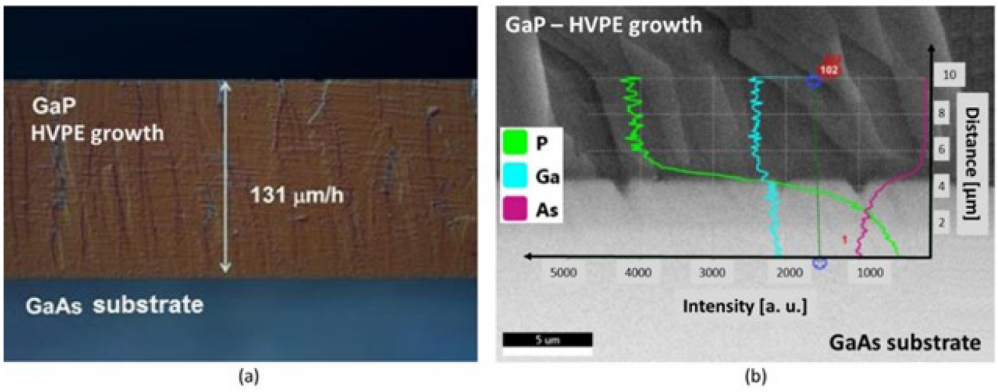

Fig. 3. Cross section of HVPE grown GaP on a GaAs substrate revealed smooth surface morphology and uniform thickness (a); Elemental profile plot across the interface, performed by EDS, indicates mutual diffusion of As (within the growing layer) and P (within the substrate) near the interface (b).

Significant improvement in the surface morphology, crystalline and optical quality of the grown material were achieved as well. An example is the near elimination of the aforementioned in § 1 absorption band between 2 and 4 μm and, in general, the increase in the IR transmission of the HVPE grown GaP. Figure 4 shows the transmission of three different GaP samples, one commercial semi-insulating (SI) GaP sample, one commercial n-type GaP substrate (before growth) and one HVPE grown GaP layer (the substrate is polished off) in the spectrum range 500 – 3300 nm.

#259429 Received 16 Feb 2016; revised 15 Apr 2016; accepted 19 Apr 2016; published 27 Apr 2016

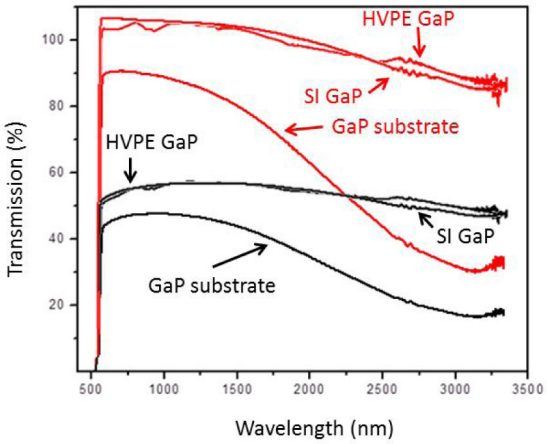

Fig. 4. IR transmittance spectra in the range 500-3300 nm of three GaP samples, one semi-insulating (SI), one commercial substrate (before growth) and one HVPE grown layer. The black lines denote the transmission with the reflection losses, while the red ones denote the corrected transmission. The GaP and SI GaP were 350 μm thick, the HVPE GaP was 370 μm thick.

The black lines in Fig. 4 denote the transmission with the reflection losses, while the red ones denote the corrected transmission after taking into account the dispersion relation of GaP in the same range (over 100% indicates size of error bars). From these graphs one can easily see that the transmission of the grown HVPE GaP is significantly improved in comparison to the commercial GaP substrate and is almost the same as the transmission in semi-insulating (SI) GaP samples. We attribute this improvement in the material optical quality, i.e. the increase of the IR transmittance and the reduction of the additional absorption band between 2 and 4 μm, to the reduction of background Si incorporation. According to [22, 23] this additional absorption band in n-type GaP is due to free carriers and Si is recognized as the primary background donor in GaP. Background Si comes from the quartz reactor parts reacting with HCl. In previous work [25] we showed that the Si concentration can be reduced by lowering the mixing zone temperature, which is accompanied by a reduction in the GaP absorption within the 2-4 μm range. More details can be found in our earlier studies [25, 28]. Other improvements that are not discussed here resulted in further improvements of the optical material quality of GaP:

In this point of view, it turned out that the heteroepitaxy (growth of GaP on GaAs) is a very practical approach for fast and easy verification of the improved IR transmission and the reduction of the additional absorption band at 2–4 μm in the HVPE grown GaP layer; because the GaAs substrate does not possess this absorption band, (see the green line in Fig. 5(a)), the transmission measurement can be done directly through both substrate and grown layer (see the blue line in Fig. 5(a)), without polishing off of the entire substrate. This cannot be avoided in the case of homoepitaxy (growth of GaP on GaP) since the commercial GaP substrate still possesses this absorption band, while the HVPE grown layer might not have it (see the red line in Fig. 5(a)). The broadband optical transmission spectra, shown in Fig. 5(a), were measured from 200 nm to 25 μm using a CARY 5000 UV-vis-NIR spectrophotometer to determine the transparency from 200 nm to 2.5 μm and a Nicolet FTIR for the range 2.5–25 μm, both with 1 nm resolution.

#259429 Received 16 Feb 2016; revised 15 Apr 2016; accepted 19 Apr 2016; published 27 Apr 2016

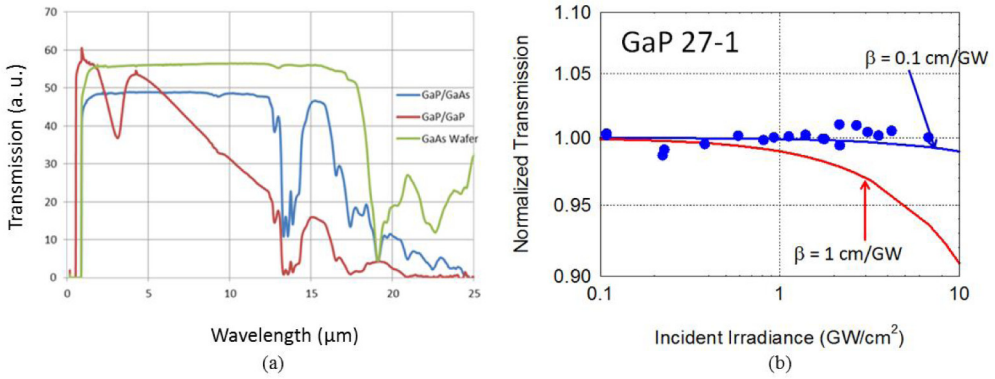

Fig. 5. IR transmittance spectra of a 350 μm thick GaAs substrate (green line), a 105-μm thick GaP HVPE grown layer on a commercial 350 μm thick GaP substrate (red line) and a 117 μm thick GaP HVPE grown layer on a 350 μm thick GaAs substrate (blue line) (a); Measurements of the 2PA at 1064 nm in 370 μm thick HVPE grown GaP (b).

Nonlinear transmission measurements were also performed on a wafer of HVPE grown GaP at 1064 nm using a laser with pulse width of 17.5 ps ($HWe^{-1}M$) and beam radius 24.7 μm ($HWe^{-2}M$). The observed transmission drop is shown in Fig. 5(b), along with the expected transmission drop [29] for a material of same thickness with 2PA coefficient β of 0.1 cm/GW and 1.0 cm/GW. The measurement indicates that at 1064 nm, the value of β for HVPE grown GaP is less than 0.1 cm/GW (vs. β = 15–16 cm/GW for GaAs). Initial measurements of the three-photon absorption (3PA) in the HVPE grown GaP were conducted at CREOL at 1300 nm using femtosecond pulsed laser. They gave no evidence of 3PA at irradiances up to 15 GW/cm^2 (3PA coefficient < 0.003 cm^3/GW^2). At this wavelength (photon energy 0.954 eV) the two-photon energy is 1.91 eV, which is below both the direct (2.78 eV) and the indirect (2.26 eV) bandgap energy. However, the three-photon energy (2.86 eV) is higher than both the indirect and the direct bandgap energy, so, in theory, 3PA is possible. However, the lack of measurable 3PA can be expected as per Ref [30].

2.3. Preparation of orientation-patterned templates

In parallel with the optimization of the growth conditions for homo and heteroepitaxy, the results from the growth experiments were also used as a feedback for the optimization of the quality of the OPGaP and OPGaAs templates. The two major techniques, the MBE-assisted polarity inversion process and the wafer bonding technique, were used for preparation of these OP templates. Commercially available GaAs and GaP wafers with thickness from 350 μm to 1000 μm were used. In general, the polarity inversion in the MBE process can be realized by the deposition of a thin intermediate layer from a closely lattice matched nonpolar material, for example, Ge for the case of OPGaAs, and Si for OPGaP. As for the wafer-bonding process, two GaP or two GaAs wafers with opposite crystallographic orientations have to be bonded via compression against each other at a temperature that is high enough to allow mutual diffusion. The major crystallographic difference between these two techniques is that the MBE process requires the usage of miscut templates whereas the wafer bonding technique can use only "on-axis" wafers. Thus all specificities for growth on "on-axis" or on miscut substrates, mentioned in § 2.2, should be taken into account when one tries to grow on wafer bonded or, resp., on MBE assisted templates. The conditions for growth of these different substrates, resp. templates, should be also different. For example, the growth on miscut substrates and from here on referred as "MBE assisted" templates can be conducted at lower supersaturation, because there are plenty of available sites on the atomic terraces. In contrast, the growths on "on-axis" substrates and from here on referred as "wafer bonded" templates will require rather higher supersaturation that is more favorable for a 2D growth,

#259429 Received 16 Feb 2016; revised 15 Apr 2016; accepted 19 Apr 2016; published 27 Apr 2016

especially when the surface crystalline quality is high. And again, because growth on an "on-axis" wafer (or a template) starts predominantly around screw dislocations, which are directly correlated to the EPD, one should also have in mind the significant difference in the EPD in the commercially available GaP and GaAs wafers (Table 1). This difference indicates that GaP wafer bonded templates will be more accommodating to 3D-growth than the GaAs ones, which means that the GaAs wafer bonded templates will provide a better start for the HVPE growth. In the case of GaP wafer bonded templates the morphology of the growing surface will deteriorate faster and, although there is not a direct correlation between the quality of the top layer surface and the domain fidelity, the chances for overgrowth of the pattern seem bigger.

Another disadvantage when bonding GaP wafers is the lack of a suitable etch-stop material, while the deposition of a thin AlGaAs or InGaAs layer can be used to determine the thickness of the inverted layer when bonding GaAs wafers. This brings the convenience of using selective wet etching followed by the photolithographic process to produce the domain pattern. In contrast, OPGaP template preparation process requires thinning of the top inverted wafer by lapping and polishing, and using a timed etch process to produce the domain pattern. It, thus, depends on a precise control of the thinning and etching processes, with the thinning step being especially labor intensive and sensitive to the polisher's experience and the specific technique. This task is made more challenging by the poor parallelism of commercially available GaP wafers, often resulting in multiple voids, shown in Fig. 6(a), between the already bonded wafers and the need to "true up" the wafers before bonding to achieve inverted layers with uniform thickness.

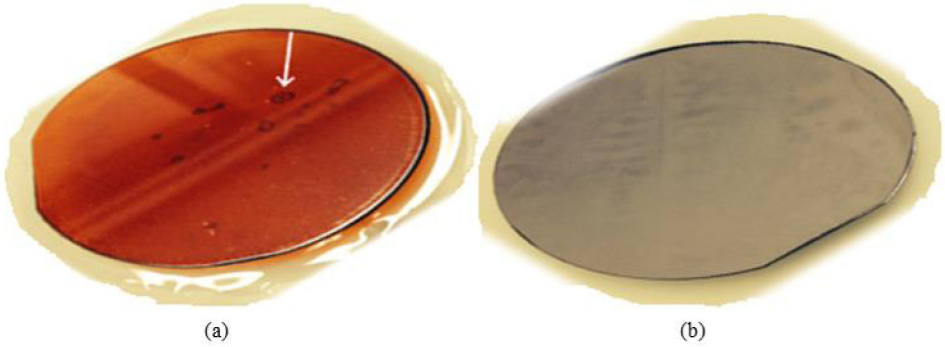

Fig. 6. Voids resulting from poor wafer parallelism when bonding GaP wafers (a); voids are rarely present when bonding GaAs wafers (b).

These problems, as Fig. 6(b) indicates, seldom occur when bonding OPGaAs templates due to the better parallelism of the commercially available GaAs wafers. GaP wafers are also 6–7 times more expensive than GaAs wafers (Table 1), which will only serve to increase the cost of the final product. More details about the wafer bonding technique for GaAs can be found in [6] and for GaP in [31, 32].

2.4. HVPE growth on orientation-patterned templates

2.4. 1. Homoepitaxial growth of OPGaP on OPGaP templates

The homoepitaxial growth experiments on both types of OP templates indicated that, if the quality of the template is good, 1– 4 hour long runs result in HVPE layers with good domain fidelity [26-Fig. 10]. However, during longer runs the top surface of the growing layer starts to get rougher and eventually the deposition overgrows the pattern [26-Fig. 11]. Such roughening has been noticed by other authors during homoepitaxy of OPGaAs [6-Fig. 3] and

#259429 Received 16 Feb 2016; revised 15 Apr 2016; accepted 19 Apr 2016; published 27 Apr 2016

OPGaP [12-Fig. 4] and [13-Fig. 3]. It was also found that overgrowth is more likely to occur when the domain period is smaller [13-Fig. 3].

Due to the fact that only "on-axis" wafers can be used in making wafer bonded templates and the lower quality of the commercial GaP wafers, which means again lower template quality and poor start for the HVPE growth, in this study we focused on preparation of OPGaAs templates with the intention to perform more heteroepitaxial growths on MBE templates.

2.4. 2. Heteroepitaxial growth of OPGaP on OPGaAs templates

Heteroepitaxial growths were performed on both MBE assisted and wafer bonded OPGaAs templates. The results from multiple experiments indicated that the domains propagate successfully following precisely the template pattern throughout the whole layer thickness and along the whole sample length (see Fig. 7), as identical growth conditions led to identical results.

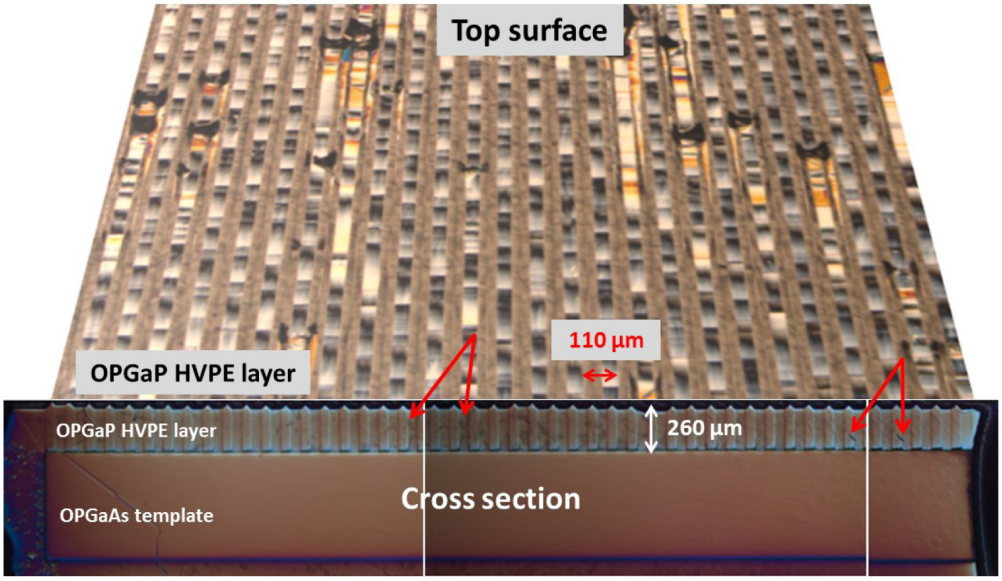

Fig. 7. A 3D-reconstruction, using microscopic images, represents the top surface (1 image) and the cross section (3 images in a row) along the whole sample length of an about 260 µm thick OPGaP layer heteroepitaxially grown on a 500 µm thick OPGaAs MBE assisted template with a pattern period of 110 µm. Each red arrow couple shows where the left image should be stitched to the next at right. The domain fidelity is excellent along the whole sample length.

Experiments with 4–8 hours durations typically resulted in up to 300–400 µm thick heteroepitaxially grown QPM structures with uniform surface morphology, high crystalline quality, excellent domain fidelity and extremely high repeatability rate. The top surface of each [100] or [$\bar{1}$00] oriented domain after up to 2–3 hours long experiments was flat packed as shown in Fig. 8(a). For longer growth durations, 4–8 hours, the [100] domains were still flat and packed with a single (100) facet, while the oppositely oriented [$\bar{1}$00] domains had rather triangularly shape packed by two $(111)_P$ facets, as shown in Fig. 8(b). In some rear cases these domains were trapezoidally shape packed by three, two $(111)_p$ and one (100), facets. The reasons for the different growth rates and top surface shapes of the two oppositely oriented domains are discussed in our earlier works [28, 32], as well by other authors. When wafer-bonded OPGaAs templates were used, the domain fidelity indicated, that further refinement of the etching and polishing procedures during the template fabrication is still necessary, as Fig. 8(c) indicates.

#259429 Received 16 Feb 2016; revised 15 Apr 2016; accepted 19 Apr 2016; published 27 Apr 2016

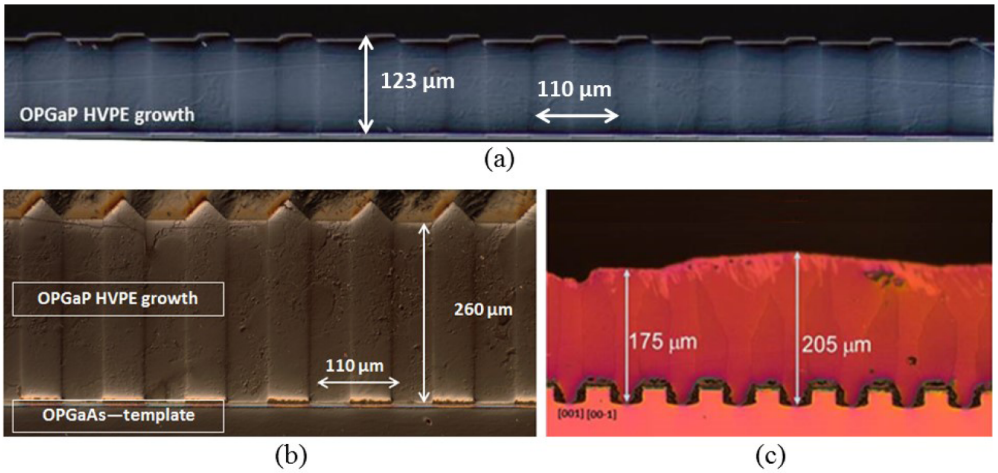

Fig. 8. Typical cross sections images of OPGaP grown by HVPE on MBE assisted polarity inversion OPGaAs templates after 2-3 hours of growth (a) and after 6-8 hours of growth (b); and OPGaP grown by HVPE on a wafer bonded OPGaAs template (c).

Reducing the growth rate and roughening of the top layer surface with the time of growth can be attributed to the parasitic nucleation that starts, probably, earlier but becomes more pronounced after the 4th hour of growth. This parasitic nucleation of GaP on the nozzle and on the reactor wall in front of the substrate produces an additional amount HCl that attacks the already grown layer (Eq. (2)):

$$GaCl + PH_3 \rightarrow GaP + HCl \qquad (2)$$

At the same time, this parasitic nucleation leads over time to an increase of the initially established V/III ratio, which is > 1 (the optimal number was V/III = 2.26). This may promote conditions for the appearance of phosphorus terminated facets, such as the $(111)_p$ facet that can lead to overgrowth of the pattern. The parasitic nucleation can be suppressed by introducing into the reactor an additional peripheral HCl flow to prevent the appearance of GaP crystallites on the quartz surfaces or, if they have already appeared, to etch them back or at least to prevent their further enlargement. However, this additional peripheral HCl may also etch back the already grown GaP layer, which means a very delicate balance is necessary. That is why in order to produce thicker OPGaP layers the crystal growers usually interrupt the process, clean the reactor, slightly polish the already grown sample (some skip this step) and perform a second growth on the same sample.

The influence of the parasitic nucleation on the growing surface morphology was also less pronounced during the heteroepitaxial growth experiments. Obviously, the higher surface quality of the GaAs wafers, relative to the GaP wafers, and the resulting higher quality of the fabricated OPGaAs templates provide conditions for a better start for the HVPE growth. As a consequence, the surface of the growing layer is not that compliant to the HCl attacks and the growth can continue uninterrupted for a longer time. One should have in mind that HCl can attack not only the existing but also create new etch-pits, i.e. new spots for nucleation on the wafer surface that could be called "secondary" nucleation. This secondary nucleation will be another reason for earlier aggravation of the layer quality. Optimization of both the growth conditions and the reactor configuration is the shortest way in suppressing the undesirable parasitic nucleation and extending the time of growth, resp. the thickness of the grown structure in one-step process.

#259429 Received 16 Feb 2016; revised 15 Apr 2016; accepted 19 Apr 2016; published 27 Apr 2016

3. Discussions

In contrast with homoepitaxial growth, the mechanism of heteroepitaxy of the III-V semiconductor materials by HVPE is not yet well-described on an atomic scale for many materials, for even traditional growth orientations [33]. The focus of this study was on heteroepitaxy of GaP on GaAs substrates and on OPGaAs templates. Thus next two critical questions had to be answered first:

1. Why can 100s of microns thick GaP films be successfully grown on GaAs at the relatively large lattice mismatch of −3.6%, while growths involving more closely lattice matched systems, for example ZnSe on GaAs [34] (only + 0.3%) have provided only limited results?

2. Does the periodic inversion of the crystalline orientation in an OP material affect the subsequent thick (homo or hetero) epitaxial growth?

Focusing on the first question, first of all we should have in mind that, if 3D-islands have been formed once, it is likely that the layer will continue growing three-dimensionally due to the Ehrlich–Schwoebel (ES) effect [35]. Namely, the ES barrier is the one that facilitates the 3D-growth by repulsing the atoms from the terrace above that are trying to cross the step to the next lower level. This barrier will increase the supersaturation there allowing the nucleation of a second layer on the top of the terrace, preventing flattening out of the 3D-island. Then by default a surface on which the EPD is greater (GaP) will result later during the growth in the appearance of a greater number of 3D-formations. Thus, such a surface will be rougher than a surface on which the initial EPD is smaller (GaAs). Although the ES barrier is relatively small, it is widely included in modeling and analysis of many morphological transformations on the growing surface [36, 37] that aim to ensure good roughness control.

At the same time, when we grow heteroepitaxially, we should have in mind that there are drastic differences in thin film growth depending on the sign of the lattice mismatch, i.e. whether the films are compressed or tensile. The reason is the anharmonicity of the interatomic potentials; the repulsive branch is much steeper than the attractive branch. Due to the smaller crystal cell of GaP the stress during the heteroepitaxial growth on a GaAs substrate will be negative, i.e. tensile. In general, when one material with a lattice constant b_0 (GaP) grows on another with a lattice constant a_0 (GaAs) and $a_0 > b_0$, misfit dislocations (MDs) that represent unsaturated (dangling) bonds, will appear originating from the material with the smaller lattice parameter (GaP) with a periodicity that is proportional to the difference $a_0 - b_0$ [38]. When this will occur, according to the misfit dislocations concept, depends on the relation between the forces that keep in place the atoms of the substrate or the atoms of the growing layer Ψ_{AA} and Ψ_{BB} and the interfacial force Ψ_{AB} [35]. In the case of GaP/GaAs $\Psi_{AB} >> \Psi_{BB}$ and $\Psi_{AB} \cong \Psi_{AA}$, which means that the growing crystal B (GaP) is homogeneously strained to fit to substrate crystal A (GaAs), i.e. the interfacial force Ψ_{AB} is strong enough to produce a pseudomorphous growth. Thus, the appearance of the expected misfit dislocations will be postponed for about 10–20 atomic monolayers, at the expense of accommodating a linearly increasing elastic strain [35]. However, beyond some critical thickness the pseudomorphous growth will become energetically unfavorable and the homogeneous strain will be released by a misfit dislocation. As a result the periodic distortion of both lattices will lead to an almost perfect match in the crystal planes in some areas, separated by stripes where the two lattices are out of registry. The key to answering the first question is that it is experimentally confirmed [39] that tensile films grow pseudomorphically up to much greater thickness compared with compressed ones at the same absolute value of the lattice mismatch (misfit). In other words, the tensile stress (the negative mismatch) favors planar growth while the compressed stress (the positive misfit) favors the formation of 3D

#259429 Received 16 Feb 2016; revised 15 Apr 2016; accepted 19 Apr 2016; published 27 Apr 2016

islands. That is why a small negative misfit is preferable [40] in the case of heteroepitaxy—indeed, in most cases of Stranski-Krastanov growth (Ge/Si, InAs/GaAs) the misfit is positive. The misfit during the above mentioned heteroepitaxy of ZnSe on GaAs [34] is also positive. To support further this statement one should have in mind that in the case of homoepitaxy the misfit is not as a default equal to zero. Crystal surfaces are as a rule under a tensile stress [41]. That is why the 2D islands forming on top should be slightly compressed. This was first noted by Frank and van der Merwe [42]. All of the above is valid for a thin film growth. In our case of thick film growth, as it was already mentioned, the misfit dislocations should be introduced beyond some critical thickness (the thickness of the pseudomorphous growth) and one can have again the usual crystal growth. However, having good quality in the beginning obviously plays an important role.

To answer the second question, one should remember that the above mentioned dangling bonds actually play an important role. For example, depending on the surface polarity of the adjacent crystal planes, the dangling bonds can act as either donors or acceptors, constituting deep energy levels in the energy gap and, thus, playing the role of recombination centers. This means that a higher dangling bond density can significantly change the properties, including the optical ones, of the material. Periodically changing the polarity in an OP material, if it is done at equal distances, statistically will strive to equalize the number of donors and acceptors. On the other hand, an alternation of the polarity on an atomic scale will entirely change the environment around the ions at the interface. This may increase the chances for the dangling bonds at least for one of the two orientations to be easier saturated, i.e. to disappear. Thus, by reducing the number of dangling bonds, the periodic alternation of the crystal polarity may have a "healing" effect on both strengthening the connection between the substrate and the growing layer and reducing the number of donors and acceptors. As far as the absorption in one material is often correlated to the presence of free carriers [26], recombination or other mechanisms or factors that reduce their number can play an important role in improving the optical quality of the material.

4. Conclusions

In summary, although GaAs remains one of the most promising QPM materials, its utility is limited by significant 2PA at wavelengths below 1.7 μm. GaP avoids this problem, but its growth remains problematic, in large part due to the poor quality of commercially available GaP wafers. Development of thick HVPE heteroepitaxial growth of GaP on GaAs, described for the first time here, allows us to combine the advantages of these two promising QPM materials while circumventing their disadvantages. This will serve to accelerate the development of frequency conversion devices based on GaP material, making them available for a wide variety of military and civilian applications.

Acknowledgments

This research was supported by the Air Force Office for Scientific Research under funding 13RY09COR. The authors are very thankful to Prof. Eric Van Stryland and Prof. David Hagan from UCF for the part of the optical measurements conducted at CREOL.

The investigations presented in this article are subject to patent protection [43–45].

#259429 Received 16 Feb 2016; revised 15 Apr 2016; accepted 19 Apr 2016; published 27 Apr 2016